

J/ψ and χ_c Polarization: theory

Hua-Sheng Shao
Peking University
PH-TH, CERN

Charmonium Workshop, LAL-Orsay

07 March 2013

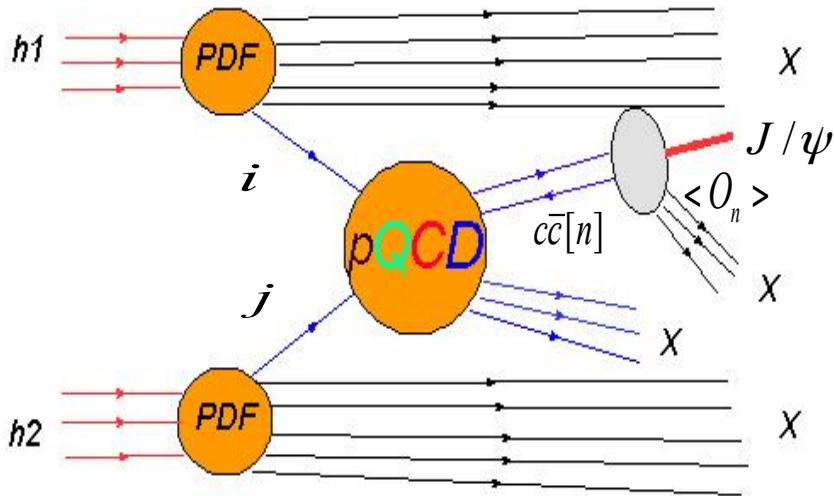
Content

- Theoretical framework: NRQCD
- J/ψ polarization and CO LDMEs fit
- X_c polarization
- Conclusion

theoretical status

- **CSM**(see e.g. [M.B.Einhorn et al. \(1975\)](#)): the heavy quark pair is produced in color-singlet states at short distance. P-wave is infrared-unsafe and incapable of interpreting heavy quarkonia production in high-pT region.
- **CEM**(see e.g. [H.Fritzsch et al. \(1977\)](#)): under the assumption of quark-hadron duality, the charm quark pair with its invariant mass between $2m_c$ and $2m_D$ evolves into charmonium. The fixed ratio of $\sigma_{J/\psi} : \sigma_{\chi_{cJ}} : \sigma_{\eta_c} : \dots$ predicted by it is in contradiction with experimental measurements.
- **NRQCD** (see e.g. [G.T.Bodwin et al. \(1995\)](#)): in addition to the color-singlet intermediate states, there are also color-octet intermediate states produced at short distance. The infrared-divergences in the color-singlet P-wave are cancelled by the CO S-wave long distance matrix elements.

factorization



- QCD factorization:

$$\sigma_{hadron} = f_{i/h1} \otimes f_{j/h2} \otimes \sigma_{parton}^{ij}$$

- NRQCD factorization [G. Bodwin et al. \(1995\)](#):

$$\sigma_{parton}^{ij} = \sigma(ij \rightarrow c\bar{c}[n] + X) \langle O_n \rangle$$

- The short distance parton level cross section is perturbative and process-dependent.
- The parton distribution functions and long distance matrix elements $\langle O_n \rangle$ are non-perturbative but universal.
- The long distance matrix elements are matrix elements of four-fermion operators in NRQCD: $\langle O_n \rangle = \langle 0 | \chi^\dagger \kappa_n \psi \left(\sum_X |H + X\rangle \langle H + X| \right) \psi^\dagger \kappa'_n \chi | 0 \rangle$
- The long distance matrix elements are scaled by v : $v_c^2 \approx 0.23, v_b^2 \approx 0.08$

Fock state

$k \backslash$	η_c, η_b	$J/\psi, \psi', \psi(3S) \dots$ $\Upsilon, \Upsilon(2S), \Upsilon(3S) \dots$	h_c, h_b	χ_{cJ}, χ_{bJ}
3	$^1S_0^{(1)}$	$^3S_1^{(1)}$	—	—
5	—	—	$^1P_1^{(1)}, ^1S_0^{(8)}$	$^3P_J^{(1)}, ^3S_1^{(8)}$
7	$^1S_0^{(8)}, ^3S_1^{(8)}, ^1P_1^{(8)}$	$^1S_0^{(8)}, ^3S_1^{(8)}, ^3P_J^{(8)}$	—	—

Color-Octet LDME(s) should be determined from experimental input.

TABLE I: Values of k in the velocity-scaling rule $\langle \mathcal{O}^Q[n] \rangle \propto v^k$ for the leading $Q\bar{Q}$ Fock states n pertinent to Q .

Challenges in P-wave !

J/ψ(ψ(2S)) polarization “anomaly”

- Although it seems to successfully explain the differential cross sections, CO encounters difficulties when the polarization is also taken into consideration.
- Dominated by gluon fragmentation to 3S_1 [8] at large p_T , LO NRQCD predicts a sizable transverse polarization, while the measurement gives almost unpolarized.
- In gluon fragmentation, the spin-flip interaction is suppressed by (Cho, Wise (1994)), and it is verified in a lattice calculation of decay matrix elements (Bodwin, et al. (2005)).

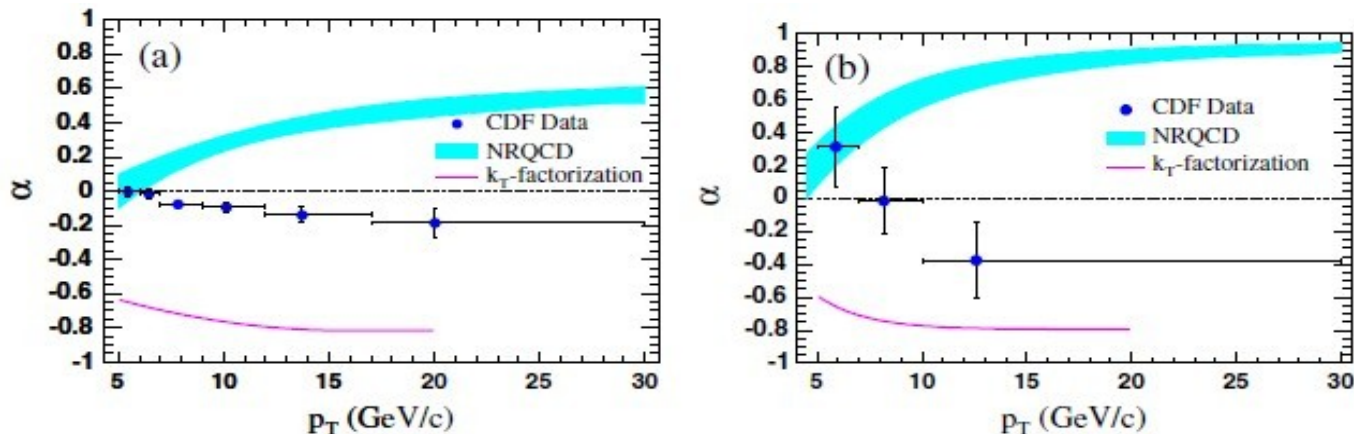


FIG. 4 (color online). Prompt polarizations as functions of p_T : (a) J/ψ and (b) $\psi(2S)$. The band (line) is the prediction from NRQCD [4] (the k_T -factorization model [9]).

A. Abulencia et al. (2007)

Large K factor in NRQCD

- The NLO color-singlet differential cross section is enhanced by 2 order relative to LO $^3S_1^{[1]}$ result at high p_T .
- On the other hand, the QCD corrections to $^3S_1^{[8]}$ channel is small.

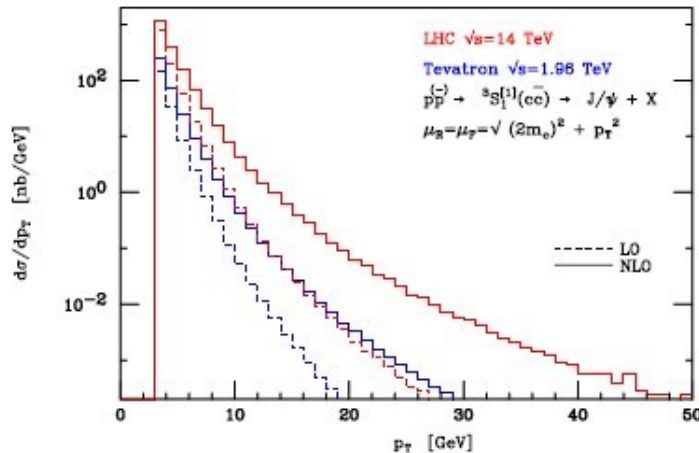


FIG. 5 (color online). Differential cross sections for direct J/ψ production via a $^3S_1^{[1]}$ intermediate state, at the Tevatron (lower histograms) and LHC (upper histograms), at LO (dashed line) and NLO (solid line). $p_T^{J/\psi} > 3$ GeV and $|y^{J/\psi}| < 3$. Details on the input parameters are given in the text.

J.M.Campbell et al. (2007)

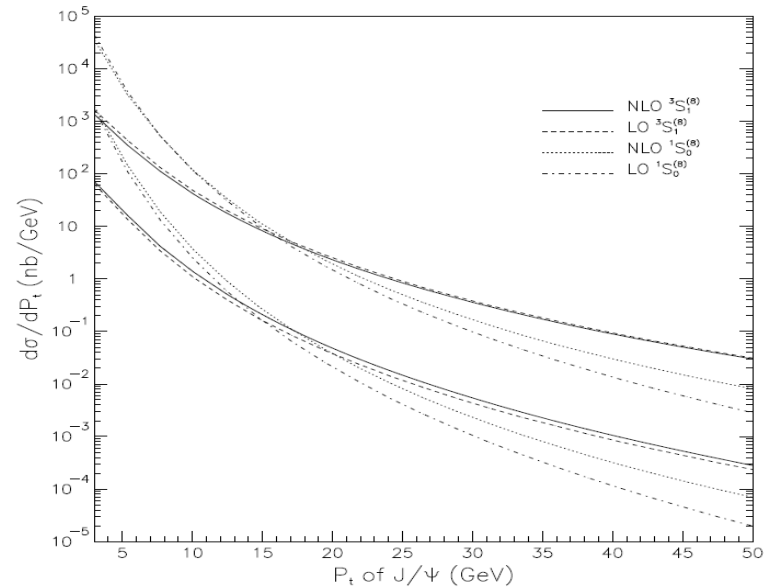
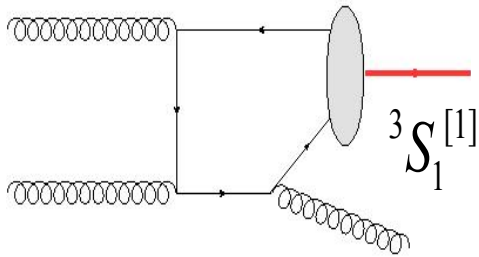


Fig. 3. Transverse momentum distribution of J/ψ production with $\mu_r = \mu_f = \mu_0$ at LHC (upper curves) and Tevatron (lower curves).

B.Gong et al. (2009)

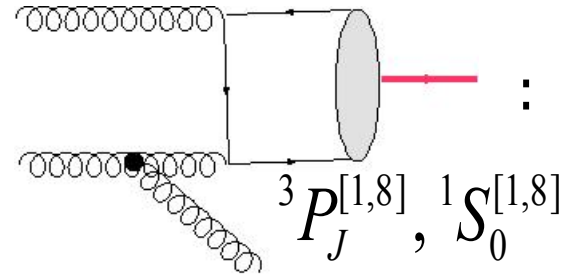
Kinematical enhancement at large PT

LO color-singlet



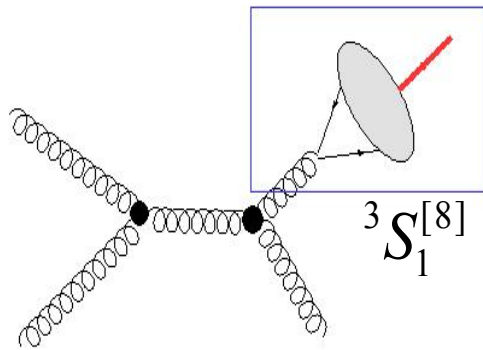
$$: \alpha_S^3 m_H^4 p_T^{-8}$$

LO color-octet



$$: \alpha_S^3 m_H^2 p_T^{-6}$$

LO color-octet

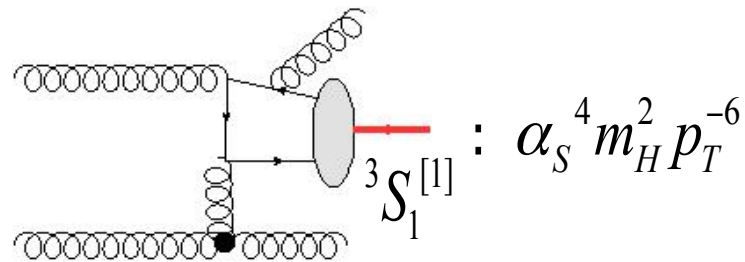


$$: \alpha_S^3 p_T^{-4}$$

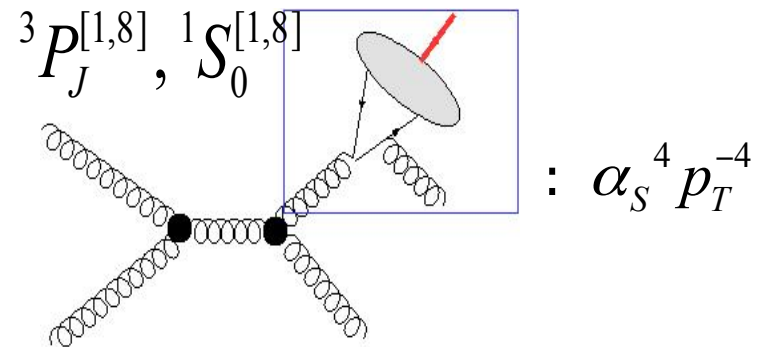
fock states	p_T scaling at LO
$^3S_1^{[1]}$	p_T^{-8}
$^3S_1^{[8]}$	p_T^{-4}
$^1S_0^{[1,8]}$	p_T^{-6}
$^3P_J^{[1,8]}$	p_T^{-6}

Kinematical enhancement at large p_T

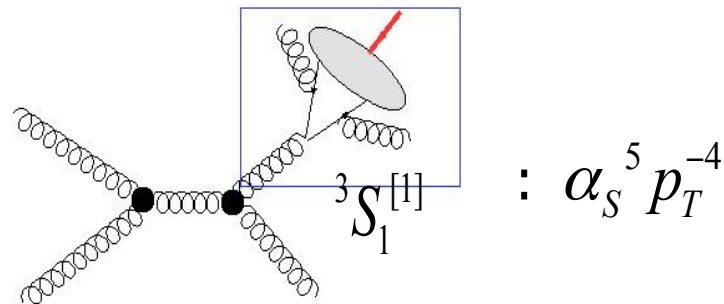
NLO color-singlet



NLO color-octet

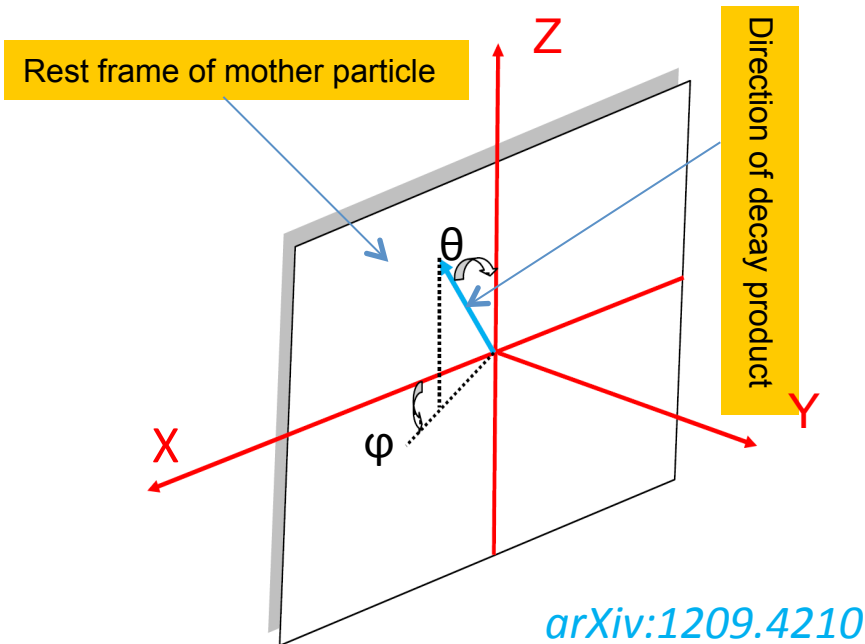


NNLO color-singlet



fock states	p_T scaling at NLO
$3S_1[1]$	p_T^{-6}
$3S_1[8]$	p_T^{-4}
$1S_0^{[1,8]}$	p_T^{-4}
$3P_J^{[1,8]}$	p_T^{-4}

Polarization observables I



2-body decay of spin-J part.

$$\frac{dN}{d\cos\vartheta} \propto 1 + \sum_{k=1}^J \lambda_{k\vartheta} \cos^{2k} \vartheta$$

1. J/ψ ($J=1$) $>$ $|+|$:-

$$\lambda_{\vartheta} = \frac{N - 3 \frac{d\sigma_{00}}{dp_T}}{N + \frac{d\sigma_{00}}{dp_T}}, N = \frac{d\sigma_{11}}{dp_T} + \frac{d\sigma_{00}}{dp_T} + \frac{d\sigma_{-1-1}}{dp_T}$$

2. $\chi c1$ ($J=1$) $>$ J/ψ γ :

$$\lambda_{\vartheta} = (1 - 3\delta) \frac{N - 3 \frac{d\sigma_{00}}{dp_T}}{(1 + \delta)N + (1 - 3\delta) \frac{d\sigma_{00}}{dp_T}}, N = \frac{d\sigma_{11}}{dp_T} + \frac{d\sigma_{00}}{dp_T} + \frac{d\sigma_{-1-1}}{dp_T}, \delta = \frac{1 + 2a_1^{J=1} a_2^{J=1}}{2}$$

E1, M2, E3

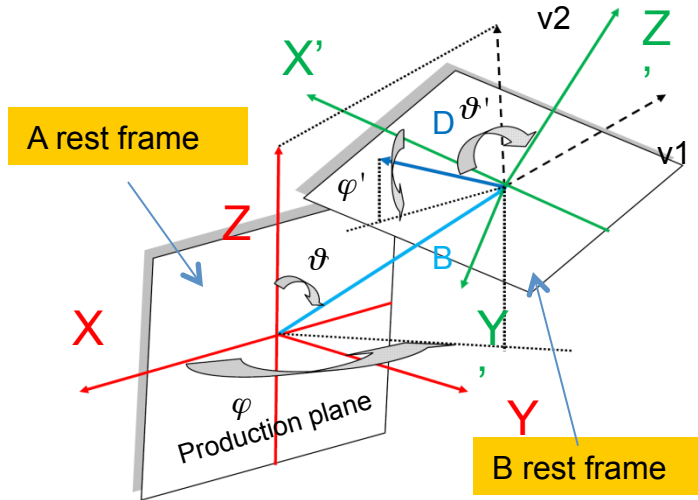
3. $\chi c2$ ($J=2$) $>$ J/ψ γ :

$$\lambda_{\vartheta} = 6 \frac{(1 - 3\delta_0 - \delta_1)N - (1 - 7\delta_0 + \delta_1) \left(\frac{d\sigma_{11}}{dp_T} + \frac{d\sigma_{-1-1}}{dp_T} \right) - (3 - \delta_0 - 7\delta_1) \frac{d\sigma_{00}}{dp_T}}{(1 + 5\delta_0 + 3\delta_1)N + 3(1 - 3\delta_0 - \delta_1) \left(\frac{d\sigma_{11}}{dp_T} + \frac{d\sigma_{-1-1}}{dp_T} \right) + (5 - 7\delta_0 - 9\delta_1) \frac{d\sigma_{00}}{dp_T}}$$

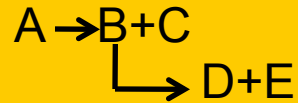
$$N = \sum_{s=-2}^2 \frac{d\sigma_{ss}}{dp_T}, \delta_0 = \frac{1 + 2a_1^{J=2} (\sqrt{5}a_2^{J=2} + 2a_3^{J=2}) + 4a_2^{J=2} (a_2^{J=2} + \sqrt{5}a_3^{J=2}) + 3(a_3^{J=2})^2}{10}$$

$$\delta_1 = \frac{9 + 6a_1^{J=2} (\sqrt{5}a_2^{J=2} - 4a_3^{J=2}) - 4a_2^{J=2} (a_2^{J=2} + 2\sqrt{5}a_3^{J=2}) + 7(a_3^{J=2})^2}{30}$$

Polarization observables II



arXiv:1209.4210



$\chi_{CJ} > J/\psi \gamma > l^+ l^- \gamma$:

$$\frac{dN}{d \cos \vartheta'} \propto 1 + \lambda_{\vartheta'} \cos^2 \vartheta'$$

1. $\chi_{C1} > J/\psi \gamma > l^+ l^- \gamma (Z'=v2)$:

$$\lambda_{\vartheta'} = (5 - 6(a_2^{J=1})^2) \frac{-N + 3 \frac{d\sigma_{00}}{dp_T}}{(15 - 2(a_2^{J=1})^2 N - (5 - 6(a_2^{J=1})^2) \frac{d\sigma_{00}}{dp_T})}$$

$$N = \frac{d\sigma_{11}}{dp_T} + \frac{d\sigma_{00}}{dp_T} + \frac{d\sigma_{-1-1}}{dp_T}$$

M2, E3 square

2. $\chi_{C2} > J/\psi \gamma > l^+ l^- \gamma (Z'=v2)$:

$$\lambda_{\vartheta'} = (7 - 14(a_2^{J=2})^2 - 5(a_3^{J=2})^2)$$

$$6N - 9 \left(\frac{d\sigma_{11}}{dp_T} + \frac{d\sigma_{-1-1}}{dp_T} \right) - 12 \frac{d\sigma_{00}}{dp_T}$$

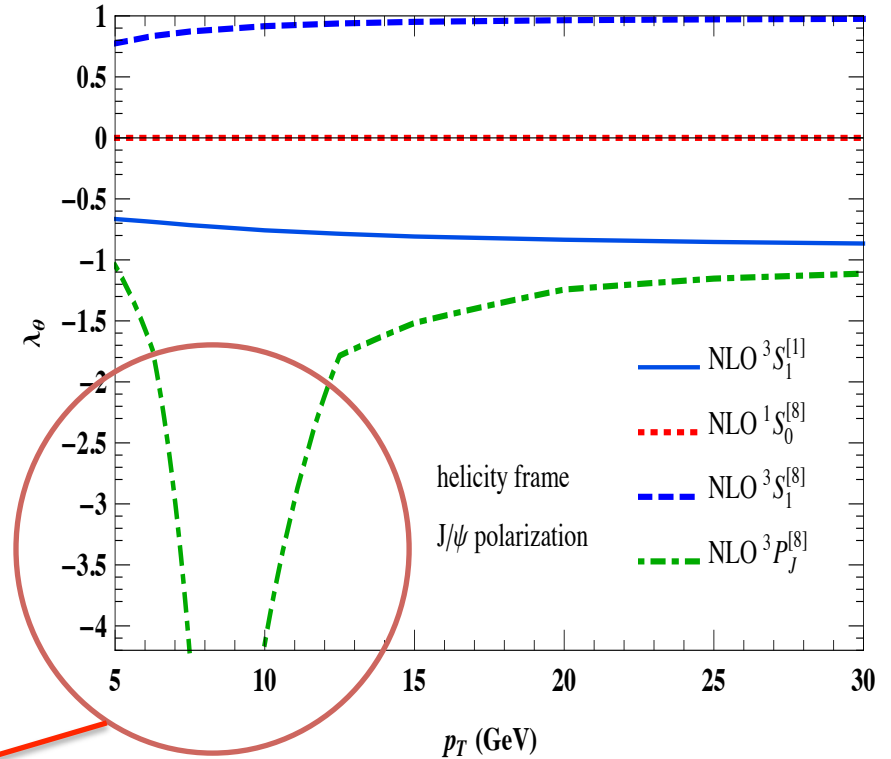
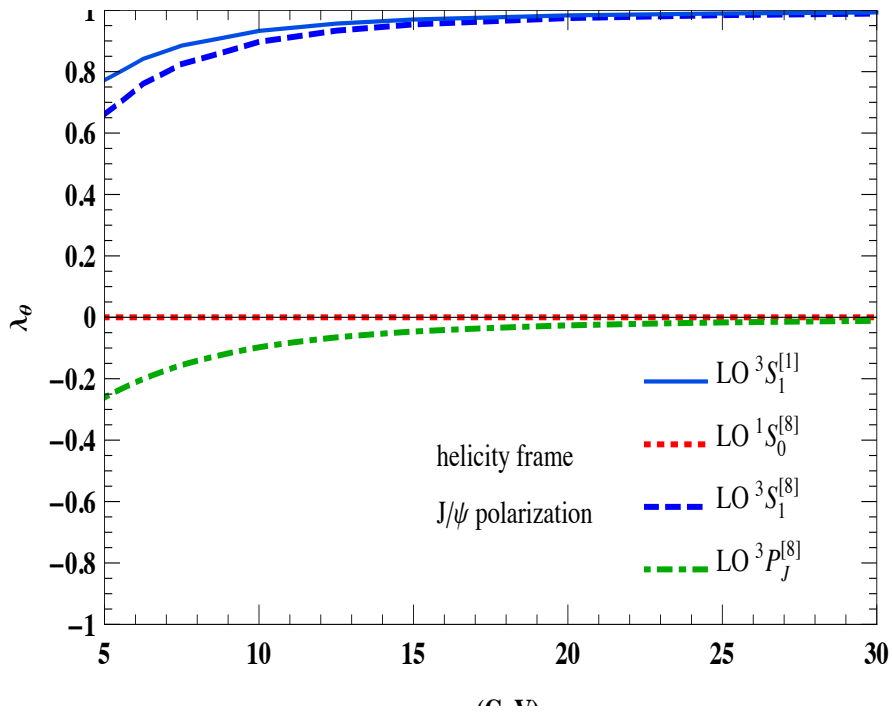
$$\frac{2(21 + 14(a_2^{J=2})^2 + 5(a_3^{J=2})^2)N + (7 - 14(a_2^{J=2})^2 - 5(a_3^{J=2})^2) \left(3 \frac{d\sigma_{11}}{dp_T} + 3 \frac{d\sigma_{-1-1}}{dp_T} + 4 \frac{d\sigma_{00}}{dp_T} \right)}{}$$

$$N = \sum_{s=-2}^2 \frac{d\sigma_{ss}}{dp_T}$$

J/ ψ Polarization

Polarization in Fock states

K.-T. Chao, Y.-Q. Ma, HSS, et al. (2012)

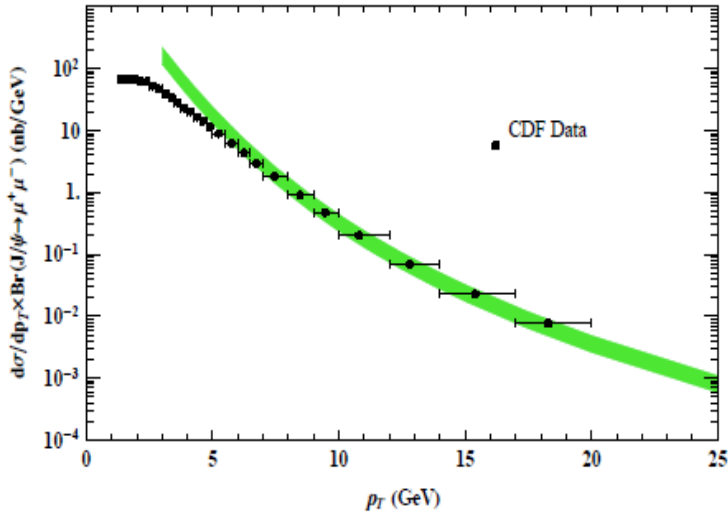


Negative !!!

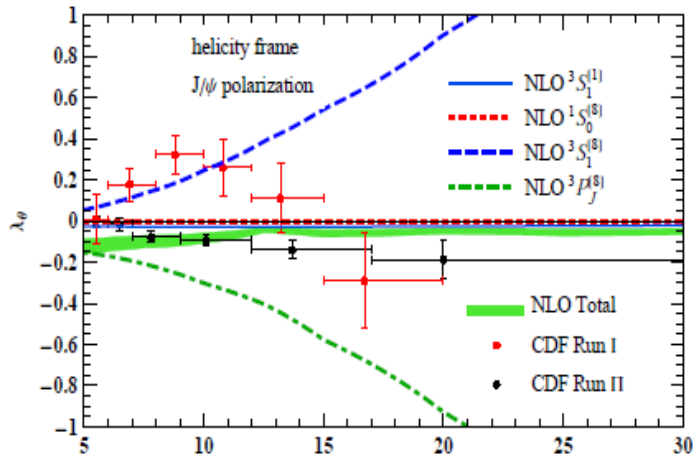
$$\mu_r = \mu_f = \sqrt{4m_c^2 + p_T^2}$$

$$\mu_\Lambda = m_c$$

CO LDMEs fit at NLO level



K.-T.Chao, Y.-Q.Ma, HSS, et al. (2012)



$$M_{0,r_0} = \langle \mathcal{O}(S_0^{[8]}) \rangle + \frac{r_0}{m_c^2} \langle \mathcal{O}(P_0^{[8]}) \rangle$$

$$M_{1,r_1} = \langle \mathcal{O}(S_1^{[8]}) \rangle + \frac{r_1}{m_c^2} \langle \mathcal{O}(P_0^{[8]}) \rangle$$

[Y.Q.Ma & K.Wang & K.T.Chao (2011)]

$\langle \mathcal{O}(S_1^{[1]}) \rangle$	M_{0,r_0}	M_{1,r_1}
GeV ³	10 ⁻² GeV ³	10 ⁻² GeV ³
1.16	7.4 ± 1.9	0.05 ± 0.02

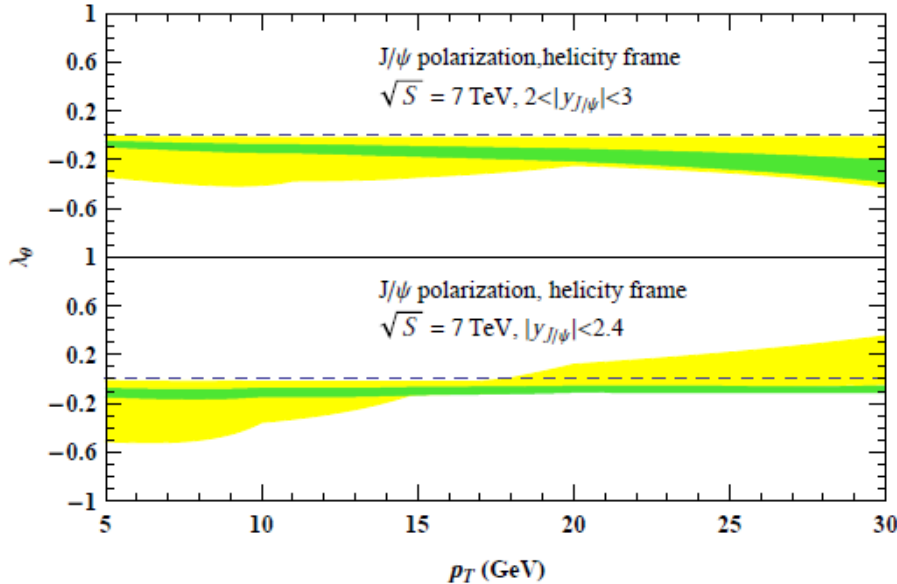
⇓ χ^2 fit to $\frac{d\sigma}{dp_T}$ and λ_θ

$\langle \mathcal{O}(S_1^{[1]}) \rangle$	$\langle \mathcal{O}(S_0^{[8]}) \rangle$	$\langle \mathcal{O}(S_1^{[8]}) \rangle$	$\langle \mathcal{O}(P_0^{[8]}) \rangle / m_c^2$
GeV ³	10 ⁻² GeV ³	10 ⁻² GeV ³	10 ⁻² GeV ³
1.16	8.9 ± 0.98	0.30 ± 0.12	0.56 ± 0.21
1.16	0	1.4	2.4
1.16	11	0	0

Hadroproduction unpolarized data can only fit two LDMEs combination unambiguously ($p_T > 7\text{GeV}$).

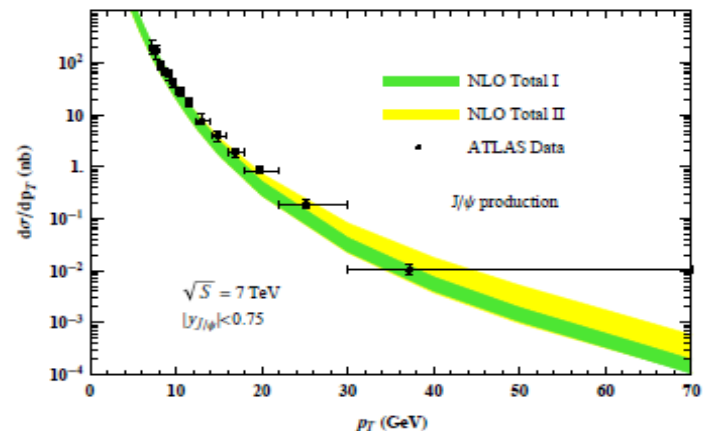
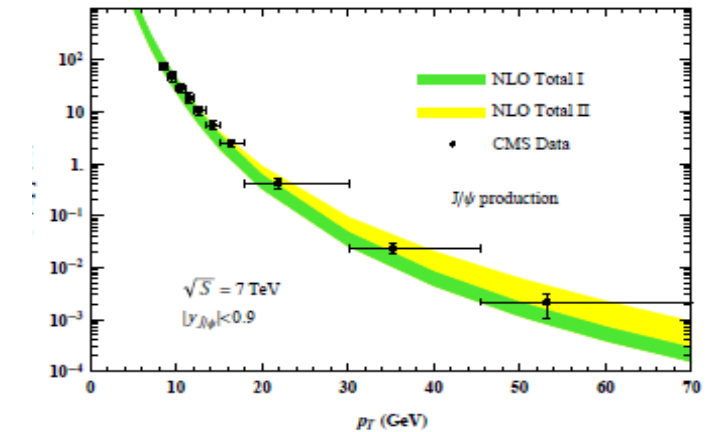
Compatible!

J/ψ polarization @LHC

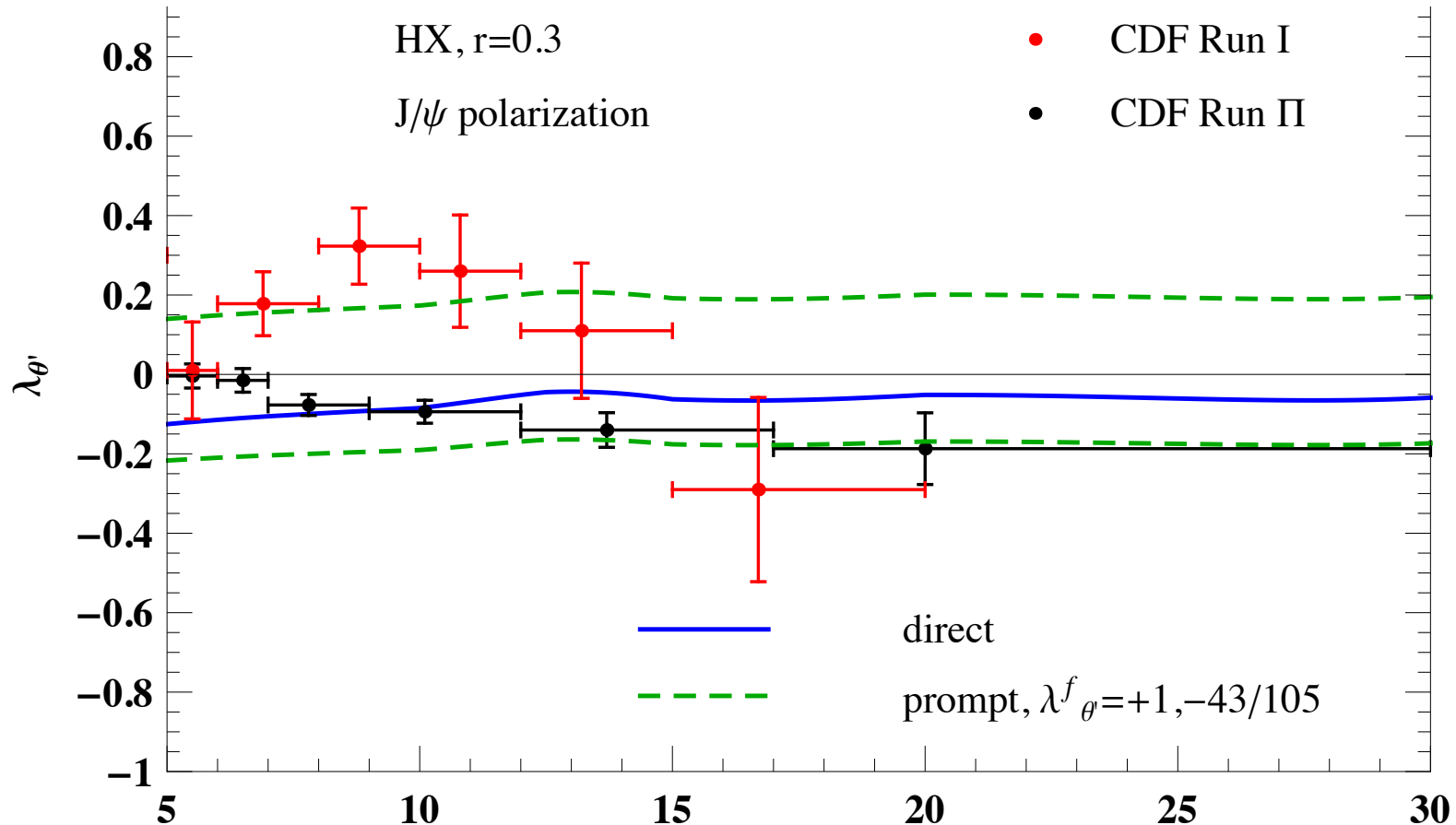


K.-T. Chao, Y.-Q. Ma, HSS, et al. (2012)

- Reasonable good for the p_T distribution of cross section up to 70 GeV at the LHC.
- To predict un-polarized results at hadron colliders, a linear combination of CO LDMEs similar to M1 should be near zero.
- Lack of feed-down contributions.



uncertainty from feeddown



1. Ignore $\psi(2S) \rightarrow J/\psi \pi \pi$.
2. Assume fraction of $\chi c \rightarrow J/\psi \gamma$ is $r = 0.3$.
3. The bound of λ_{θ} of J/ ψ from χc is $-43/105 \sim 1$.

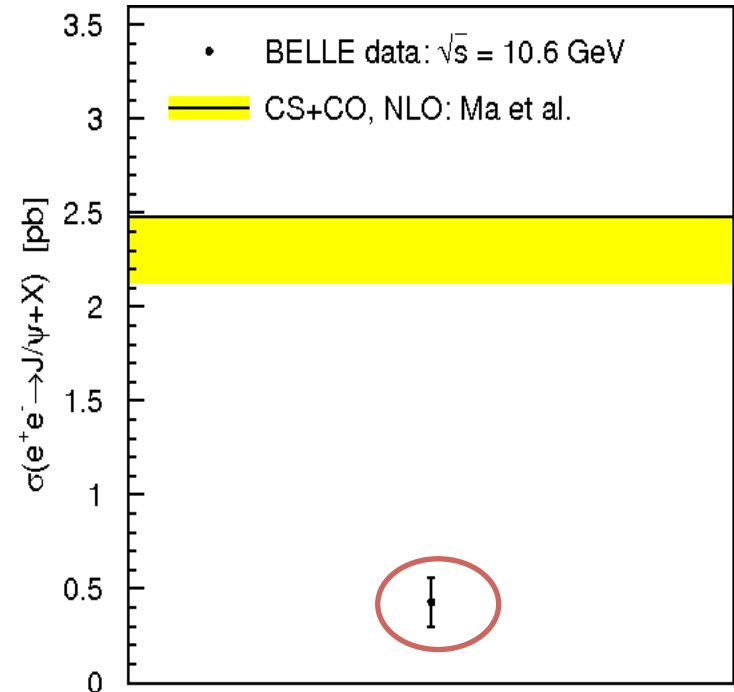
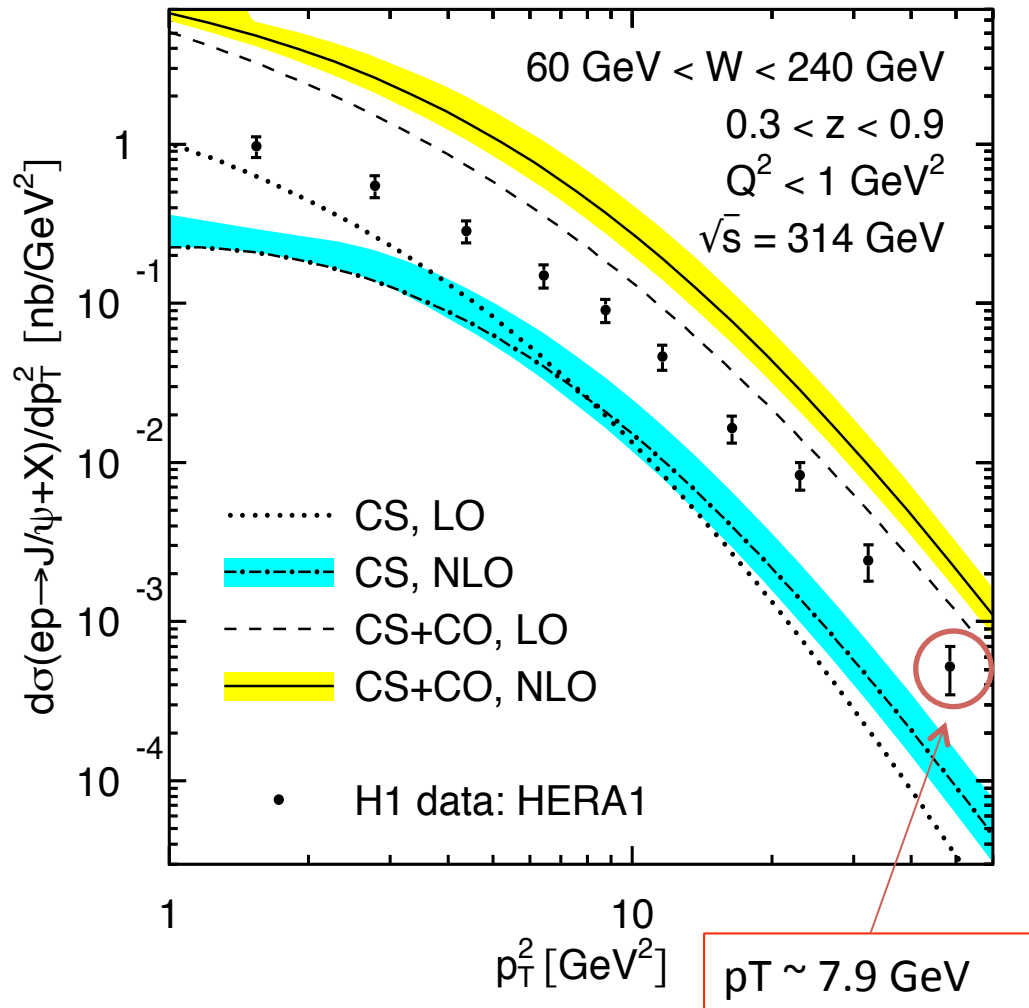
advantages

- 1. The unpolarized predictions at hadron colliders (RHIC, Tevatron I, II and LHC) are quite good with data when $p_T > 7$ GeV (cutoff in fit).
- 2. Positive P-wave CO LDME makes the polarization at hadron colliders near zero, i.e. unpolarized. It is quite close to CDF Run II data though it is lack of feeddown.

disadvantages

- 1. It cannot predict $p_T < 7$ GeV hadroproduction data, and it is also far from HERA data (p_T is also small) and BELLE data. It might be debited to the failure of factorization of NRQCD in this small p_T regime(?).
- 2. Resummation of large logarithm at large p_T regime might make the good prediction worse.
- 3. It is still lacking of feeddown contribution in polarization. However, it might be not so important as long as P-wave CO LDME positive.

H1 data and BELLE data



Stole from M. Butenschon's talk

M. Butenschon and B. Kniehl's fit

M. Butenschon, B. Kniehl, (2011)

- 1. Use unpolarized data in **pp** (not include ATLAS and CMS large pT data), **$\gamma p, \gamma\gamma$** and **$e+e-$** collisions.

- 2. $p_T > 1$ GeV for **$\gamma p, \gamma\gamma$** data and $p_T > 3$ GeV for

pp. There is only one data for **$e+e-$** .

$$\langle O^{J/\Psi} (^1S_0^{[8]}) \rangle = (4.97 \pm 0.44) \times 10^{-2} \text{ GeV}^3, \langle O^{J/\Psi} (^3S_1^{[8]}) \rangle = (2.24 \pm 0.59) \times 10^{-3} \text{ GeV}^3,$$

$$\langle O^{J/\Psi} (^3P_0^{[8]}) \rangle = (-1.61 \pm 0.20) \times 10^{-2} \text{ GeV}^5$$

- 3. After feeddown was included (pp:36%, γp : 15%, $\gamma\gamma$: 9%, $e+e-$: 26%),

$$\langle O^{J/\Psi} (^1S_0^{[8]}) \rangle = (3.04 \pm 0.35) \times 10^{-2} \text{ GeV}^3, \langle O^{J/\Psi} (^3S_1^{[8]}) \rangle = (1.68 \pm 0.46) \times 10^{-3} \text{ GeV}^3,$$

$$\langle O^{J/\Psi} (^3P_0^{[8]}) \rangle = (-9.08 \pm 1.61) \times 10^{-3} \text{ GeV}^5$$

advantages

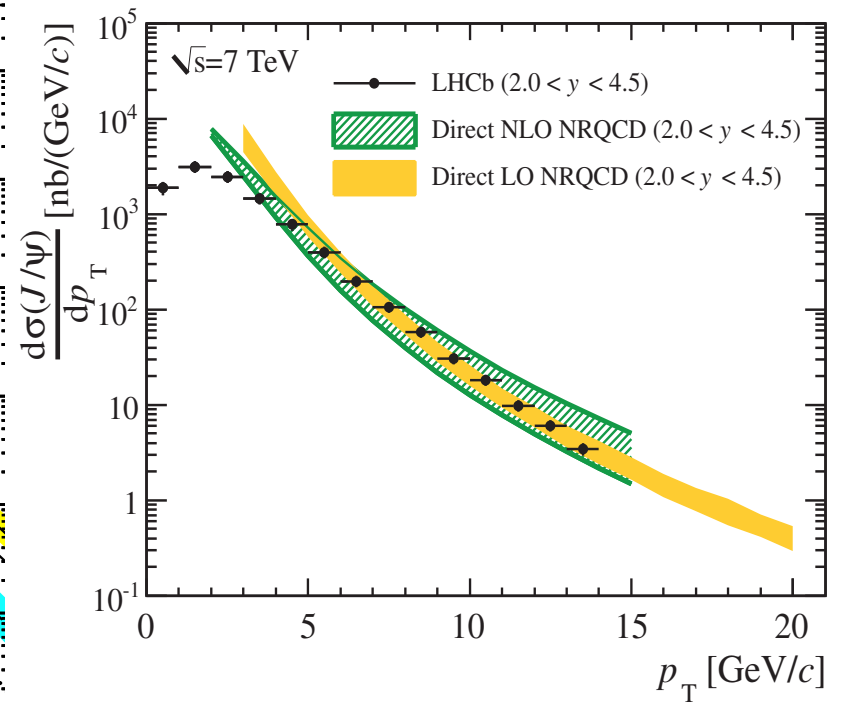
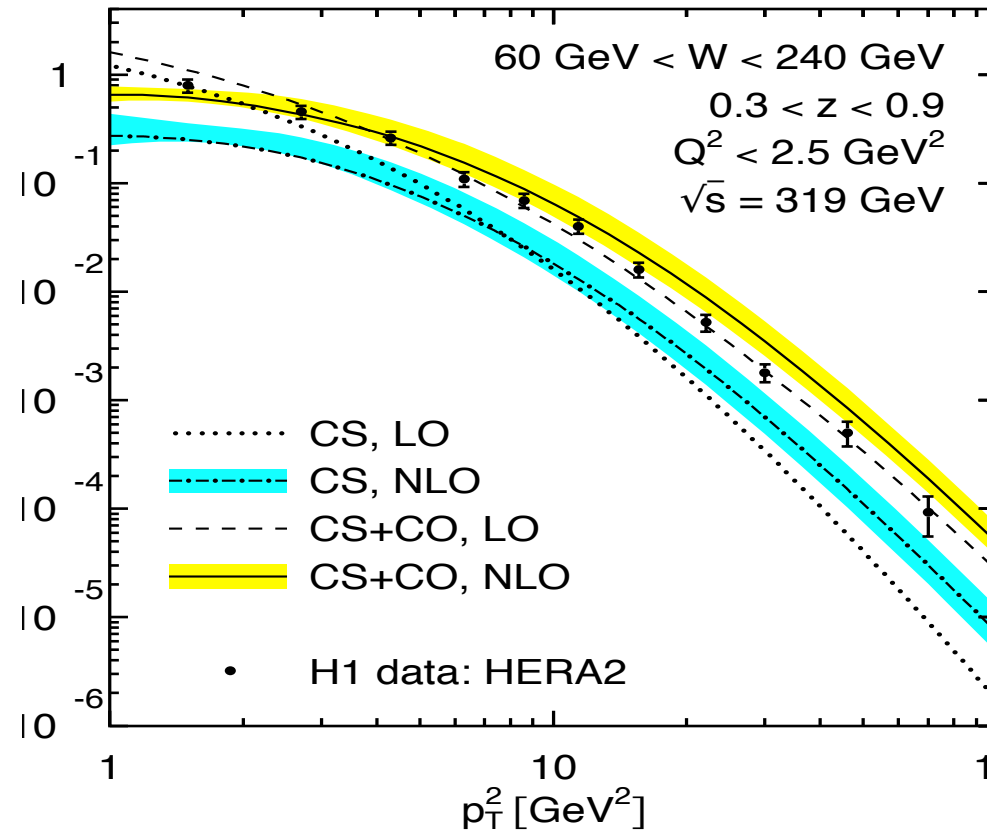
- 1. They include more small p_T data in their fit ($p_T > 3$ GeV for hadroproduction and $p_T > 1$ GeV for photoproduction and two-photon production). They can describe small p_T hadroproduction data and HERA data better.
- 2. The discrepancy of e^+e^- data and NRQCD prediction is much smaller.

disadvantages

- 1. Some discrepancies like H1 data, LHCb data are still there with BK's global fit.
- 2. ATLAS and CMS's large p_T data are not included. The prediction of unpolarized p_T spectrum at large p_T is above the experimental data (a factor of $3\sim 4$). It might be better after including resummation of logs of m_c/p_T . Can resummation change so much?
- 3. Because the value of P-wave CO LDME is negative, cancellation with S-wave CO cannot happen. It predicts transverse polarization at CDF Run II, which is in conflict (It is also lacking of feeddown in polarization).

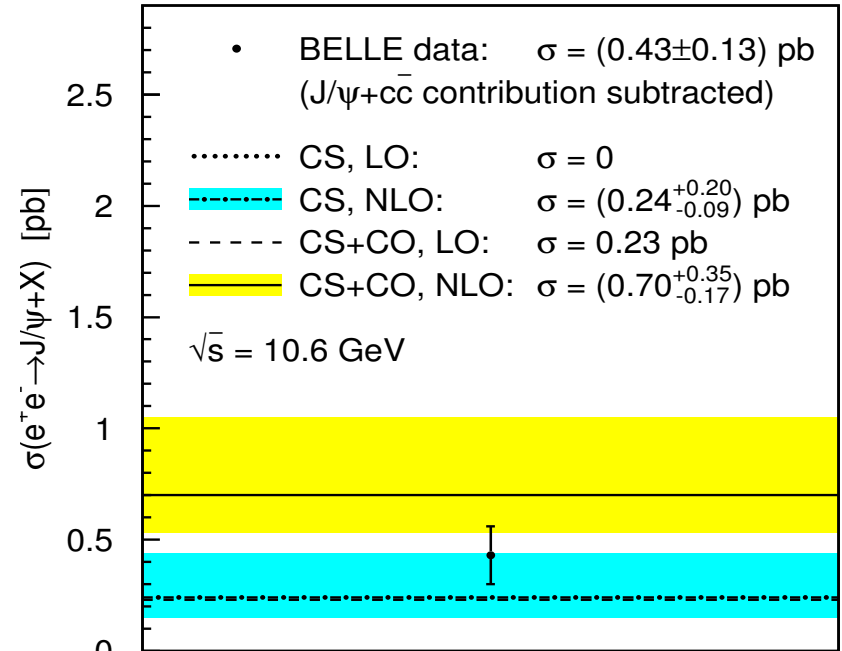
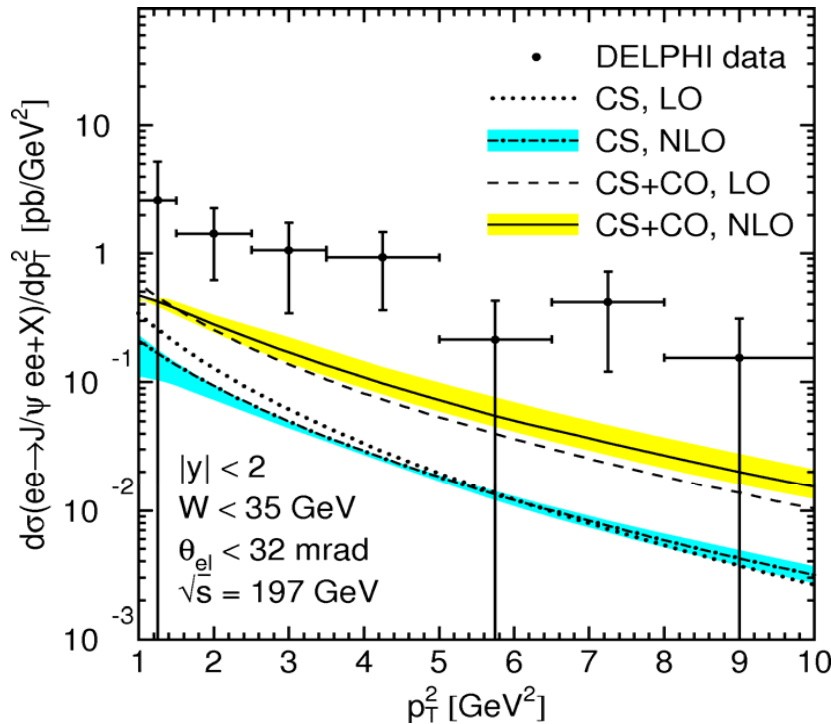
H1 data and LHCb data

M. Butenschon, B. Kniehl, (2011)



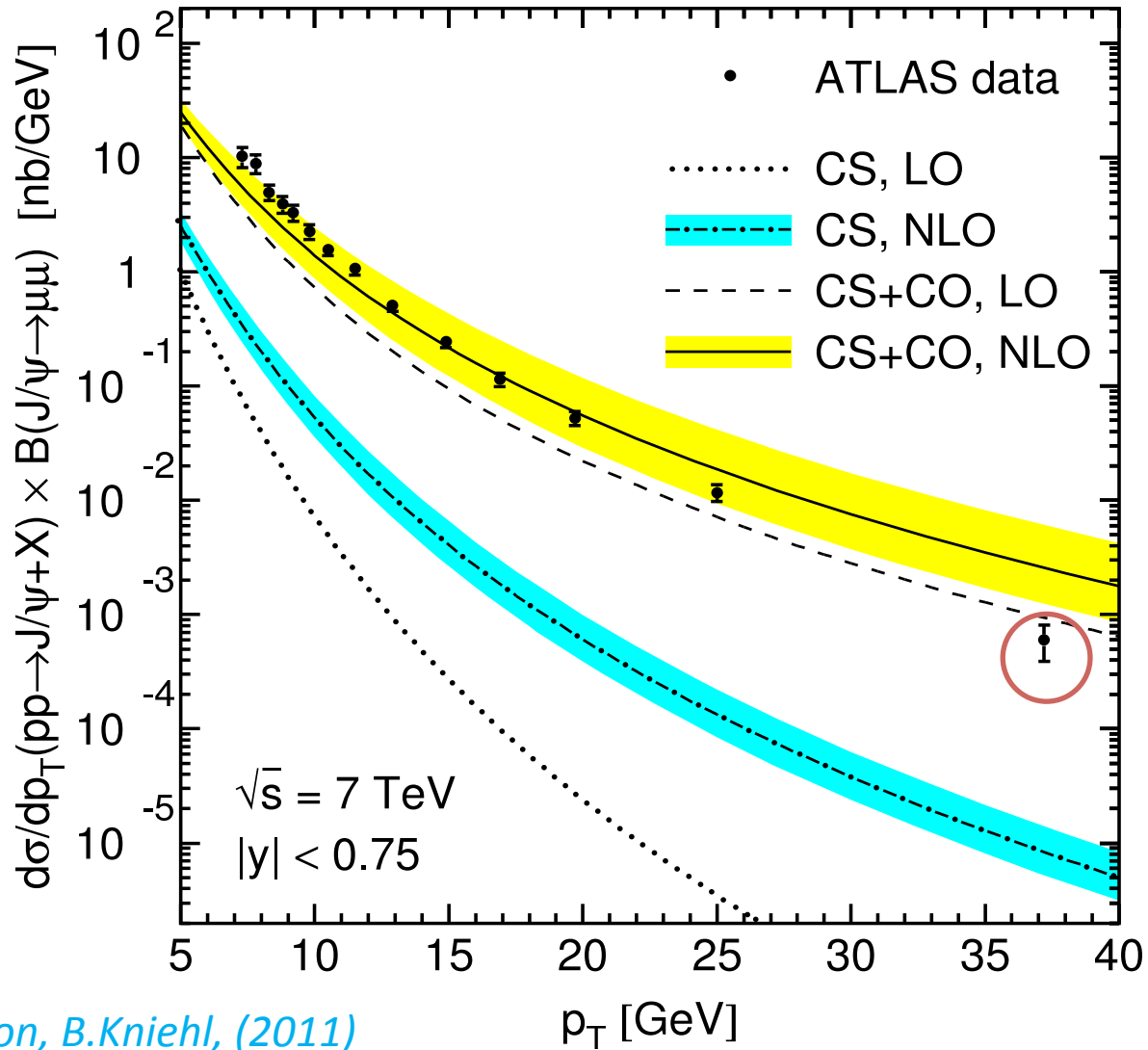
DELPHI data and BELLE data

M. Butenschon, B. Kniehl, (2011, 2012)



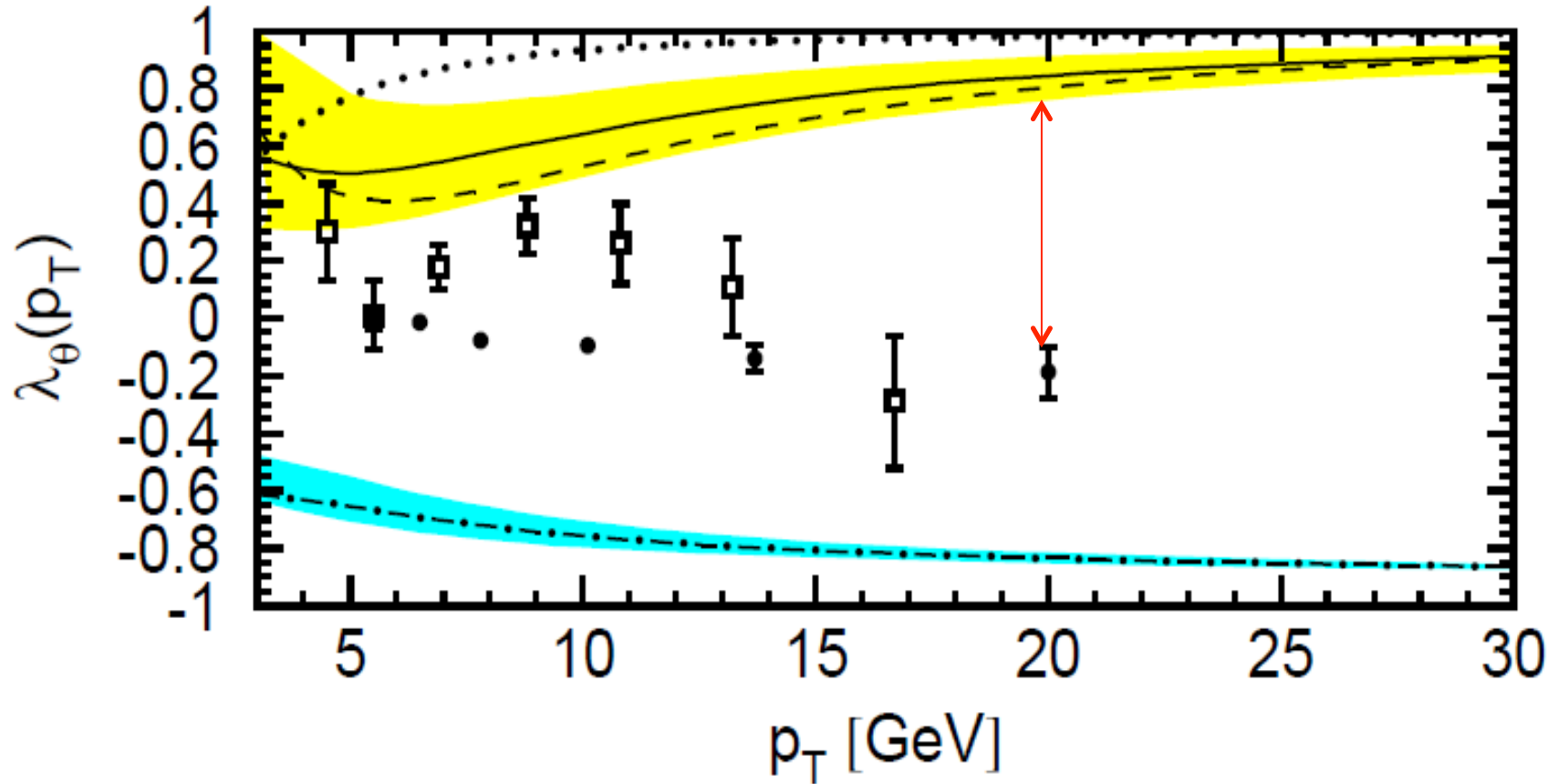
Factorization of NRQCD might be violated at such small p_T ? !

ATLAS data



Polarization @CDF Run II

M.Butenschon, B.Kniehl, (2012)



fit by BWWZ group

B.Gong, L.-P.Wan, J.-X.Wang, H.-F.Zhang (2012)

- 1. Use unpolarized data and fit central region data by CDF Run II and forward region data by LHCb simultaneously (r0 and r1 in M0 and M1 are slightly different in these two regions!!!).
- 2. $p_T > 7 \text{ GeV}$.
- 3. Include feeddown from χ_c and $\Psi(2S)$.

$$\begin{aligned}\langle O^{J/\Psi}({}^1S_0^{[8]}) \rangle &= 0.097 \pm 0.009 \text{ GeV}^3, \langle O^{J/\Psi}({}^3S_1^{[8]}) \rangle = (-0.46 \pm 0.13) \times 10^{-2} \text{ GeV}^3, \\ \langle O^{J/\Psi}({}^3P_0^{[8]}) \rangle &= (-0.0214 \pm 0.0056) \text{ GeV}^5, \langle O^{\Psi'}({}^1S_0^{[8]}) \rangle = (-0.012 \pm 0.869) \times 10^{-2} \text{ GeV}^3, \\ \langle O^{\Psi'}({}^3S_1^{[8]}) \rangle &= (0.34 \pm 0.12) \times 10^{-2} \text{ GeV}^3, \langle O^{\Psi'}({}^3P_0^{[8]}) \rangle = (0.945 \pm 0.54) \times 10^{-2} \text{ GeV}^5, \\ \langle O^{\chi_c^0}({}^3S_1^{[8]}) \rangle &= (0.22 \pm 0.012) \times 10^{-2} \text{ GeV}^3\end{aligned}$$

Cancellation is not sufficient to give an unpolarized prediction.

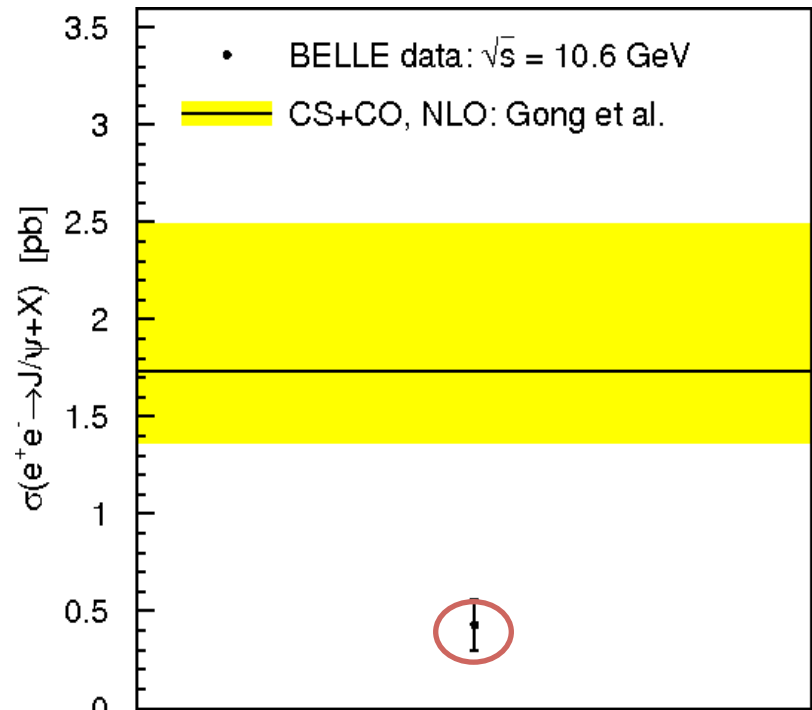
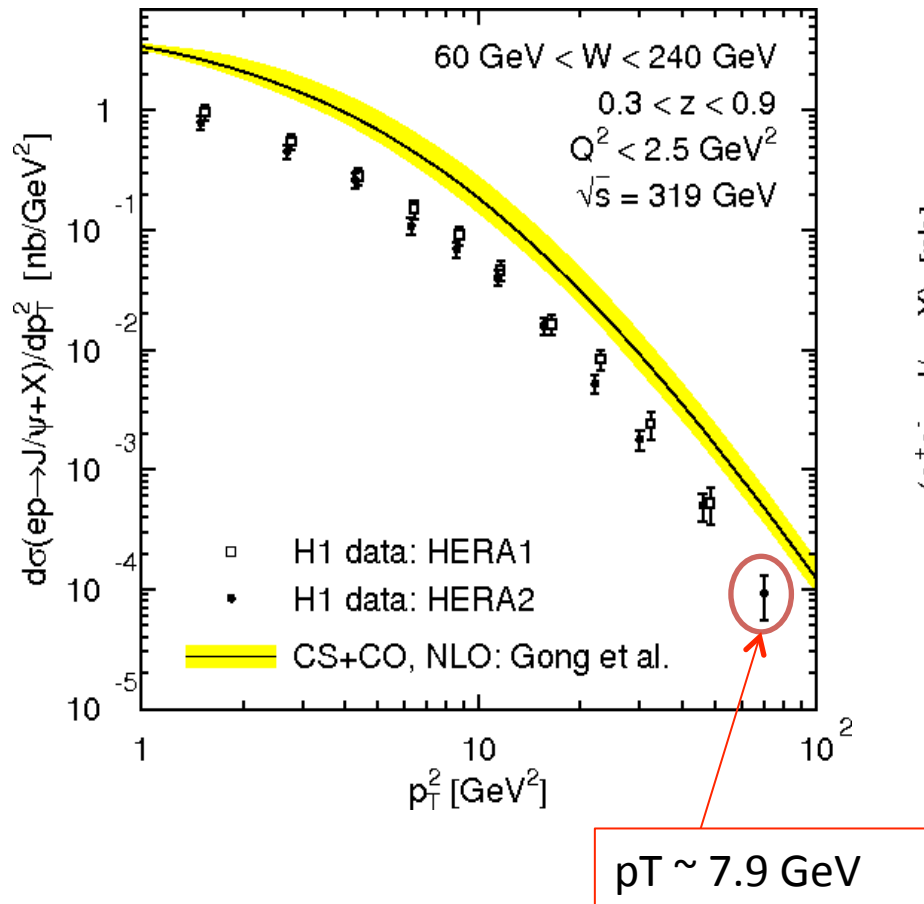
advantages

- 1.They fit J/ψ CO LDMEs after subtracting χ_c and $\psi(2S)$ feeddown for the first time.
- 2.They extract three CO LDMEs only from the hadroproduction data.
- 3. The cancellation of P-wave and S-wave makes the polarization prediction is better than BK's prediction at CDF Run II.

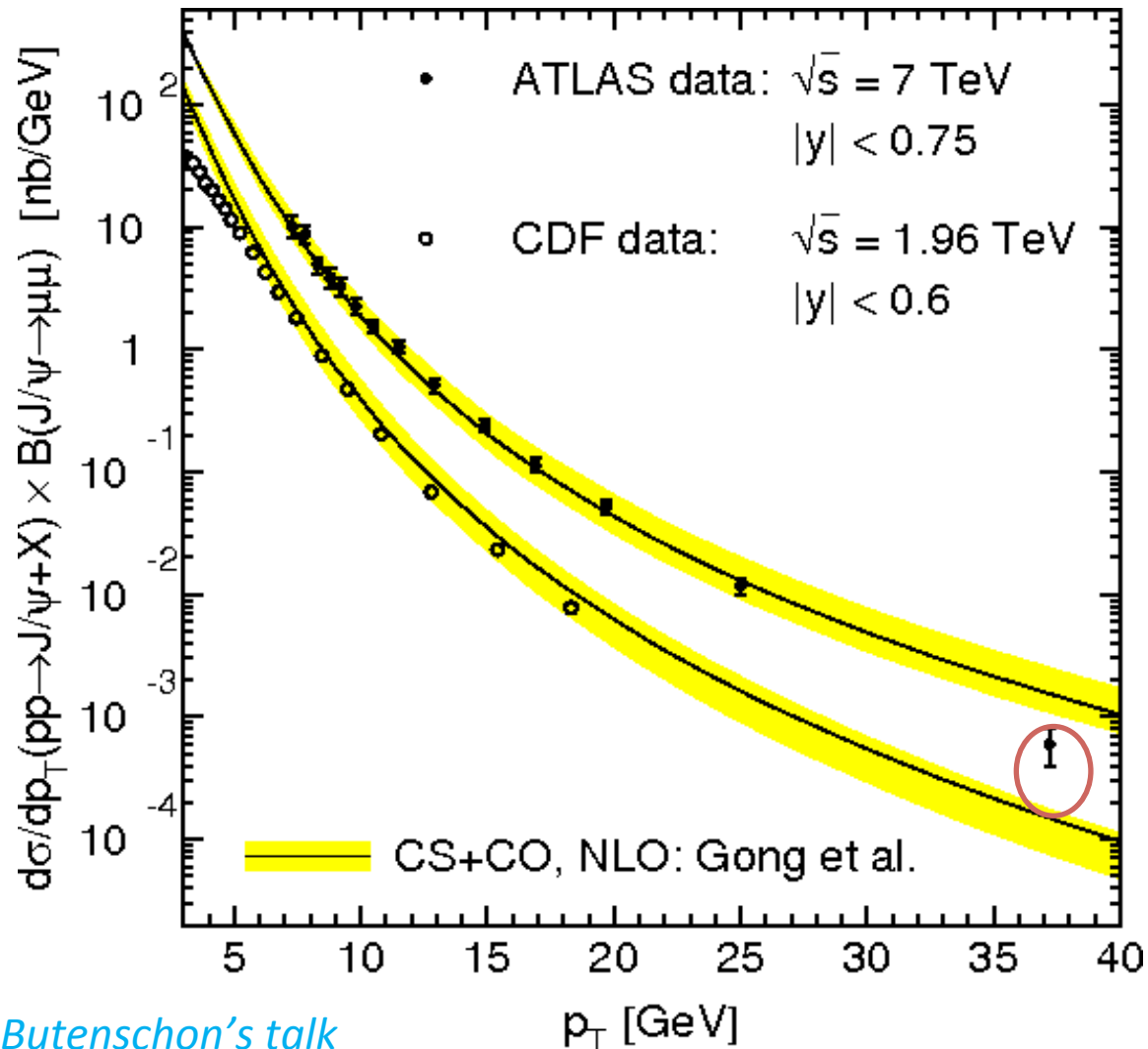
disadvantages

- 1. The main difference with CMSWZ and BK is from direct part (the feeddown contribution is not so important). It is a compromise set between CMSWZ and BK's sets. They are in disagreement with HERA and BELLE data.
- 2. There is a **slight** difference between their prediction and large p_T data (CMS and ATLAS). Resummation ??
- 3. Because the cancellation is not sufficient, it is still predicting a transverse polarization, which is in contrast with CDF Run I and II data.

H1 data and BELLE data

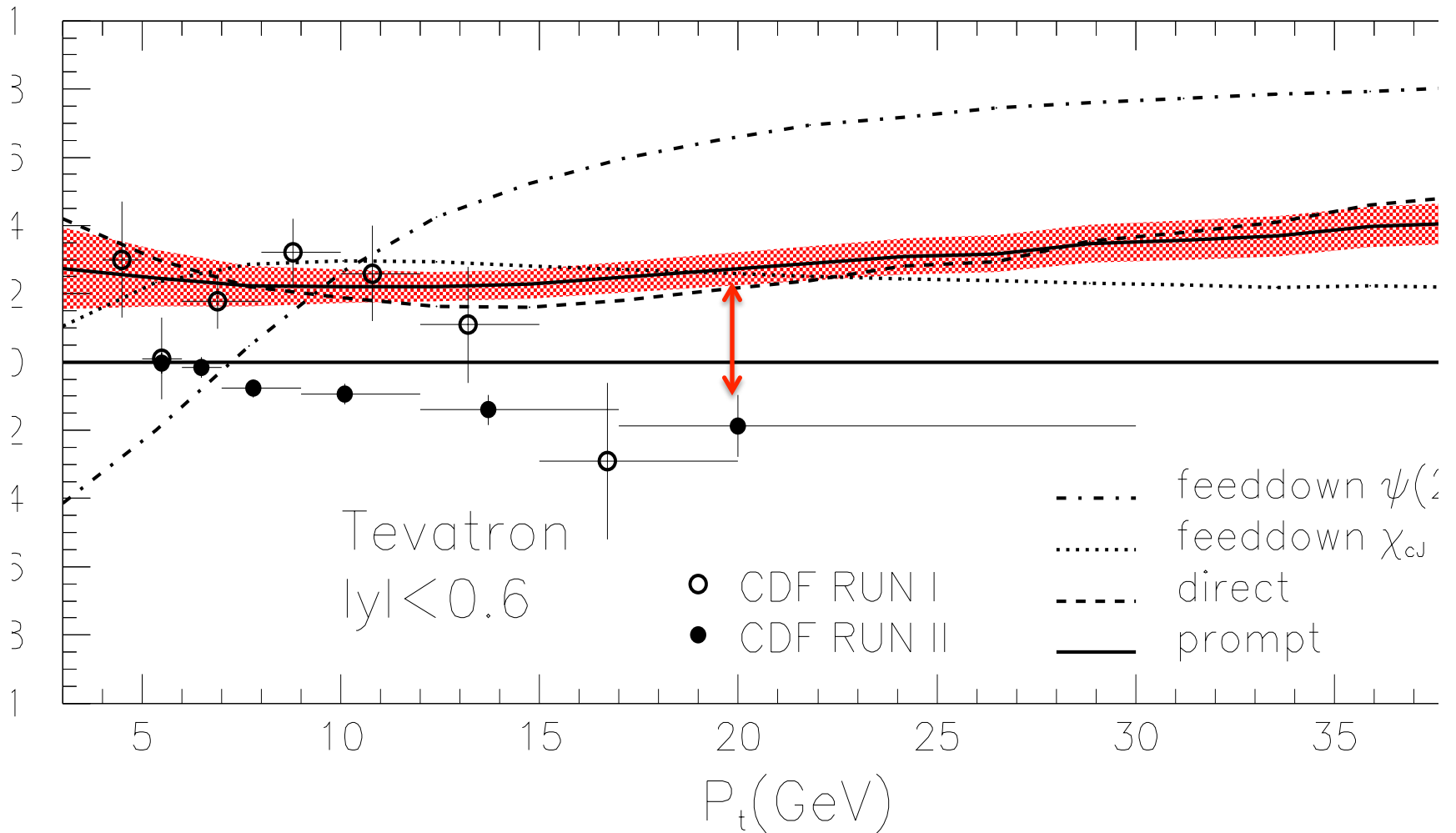


ATLAS data



Stole from M. Butenschon's talk

polarization@CDF Run II



χ_c Polarization

normalized multipole amplitudes

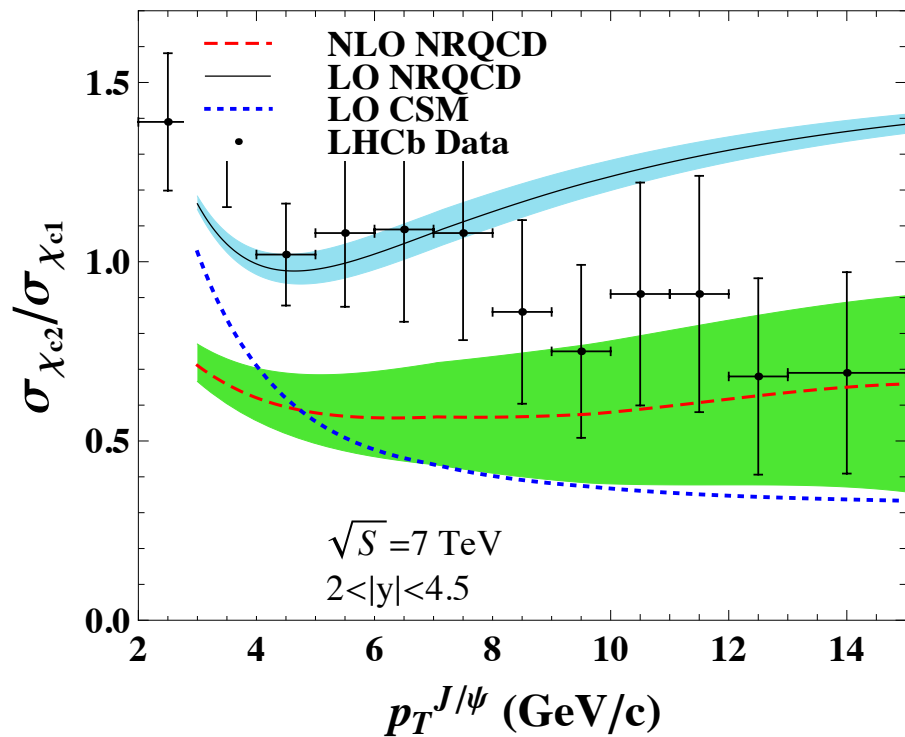
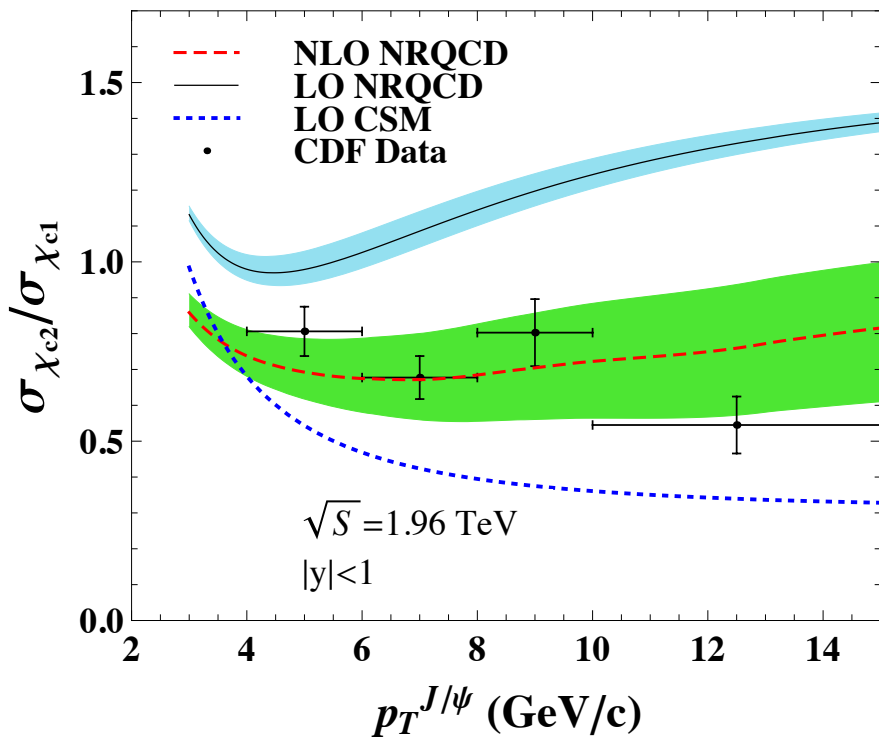
Experiment	$a_2^{J=1} (10^{-2})$
CLEO[26]	$-6.26 \pm 0.63 \pm 0.24$
Crystal Ball [27]	$-0.2^{+0.8}_{-2.0}$
E835 [29]	$0.2 \pm 3.2 \pm 0.4$

Experiment	$a_2^{J=2} (10^{-2})$	$a_3^{J=2} (10^{-2})$
CLEO(Fit 1)[26]	$-9.3 \pm 1.6 \pm 0.3$	0(fixed)
CLEO(Fit 2)[26]	$-7.9 \pm 1.9 \pm 0.3$	$1.7 \pm 1.4 \pm 0.3$
Crystal Ball [27]	$-33.3^{+11.6}_{-29.2}$	0(fixed)
E760(Fit 1) [28]	-14 ± 6	0(fixed)
E760(Fit 2) [28]	-14^{+8}_{-7}	0^{+6}_{-5}
E835(Fit 1) [29]	$-9.3^{+3.9}_{-4.1} \pm 0.6$	0(fixed)
E835(Fit 2) [29]	$-7.6^{+5.4}_{-5.0} \pm 0.9$	$2.0^{+5.5}_{-4.4} \pm 0.9$

Our choice !

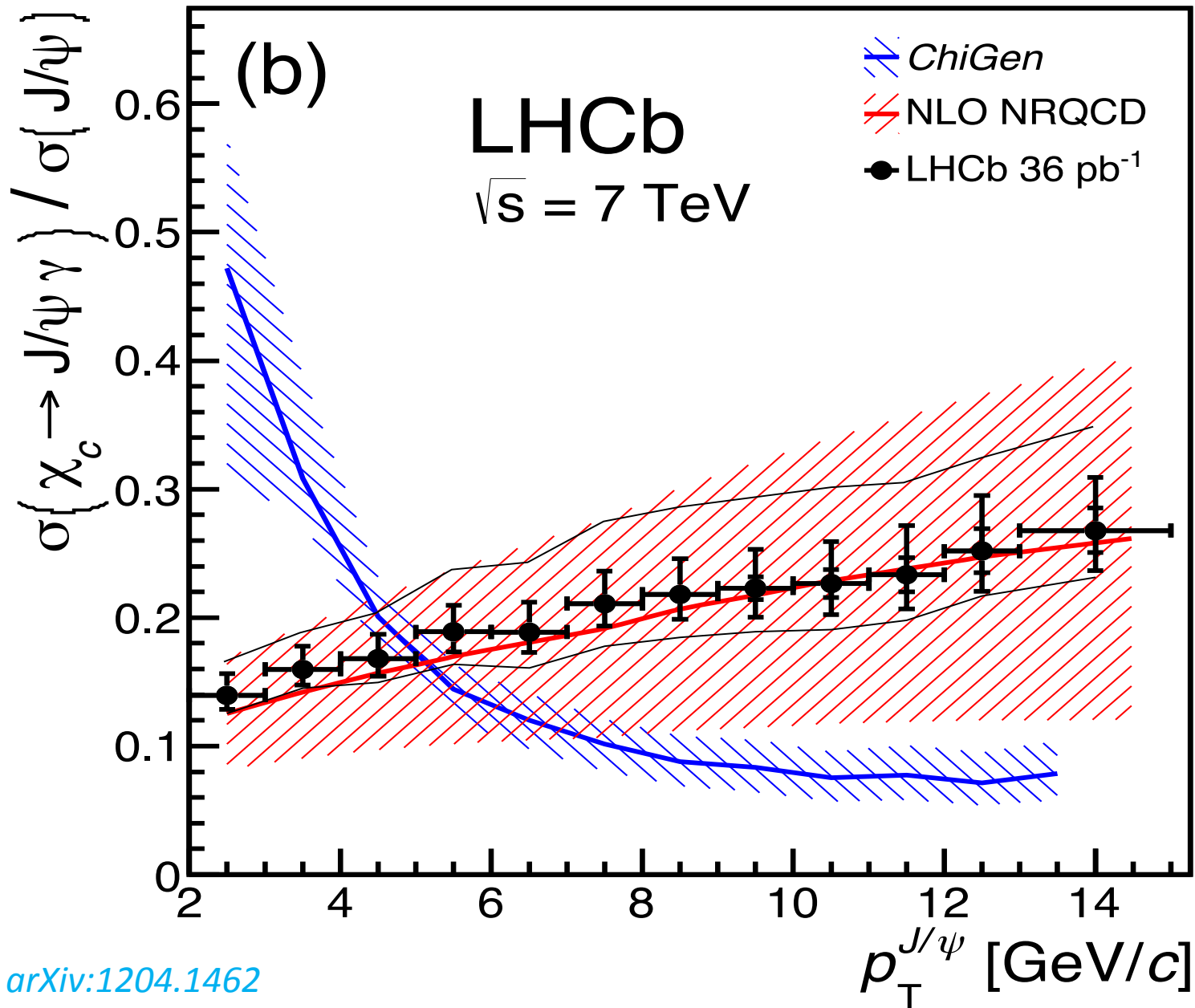
Single quark radiation

Ratio and LDMEs



$$\langle O^{\chi_{cJ}}(^3S_1^{[8]}) \rangle = (2J+1) \times (2.2_{-0.32}^{+0.48}) \times 10^{-3} \text{ GeV}^3$$

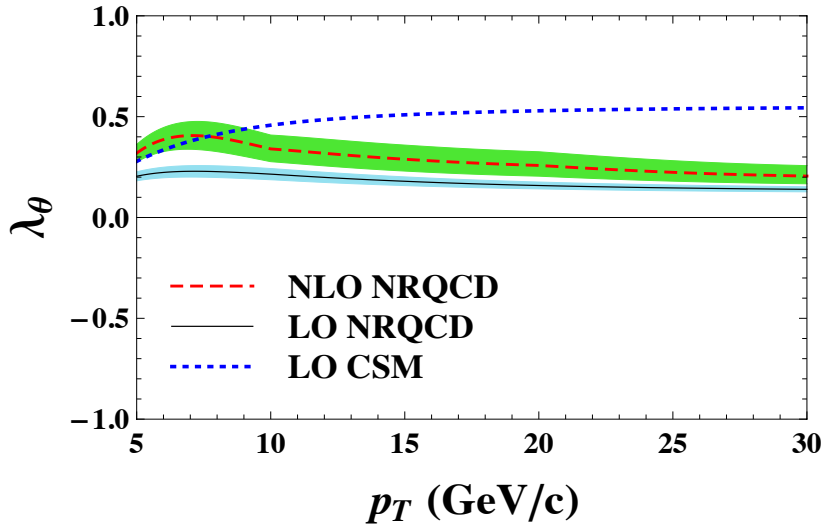
$$\langle O^{\chi_{cJ}}(^3P_J^{[1]}) \rangle = (2J+1) \frac{3N_c |R'(0)|^2}{2\pi}, |R'(0)|^2 = 0.075 \text{ GeV}^5$$



$\chi_{cJ} > J/\psi \gamma$

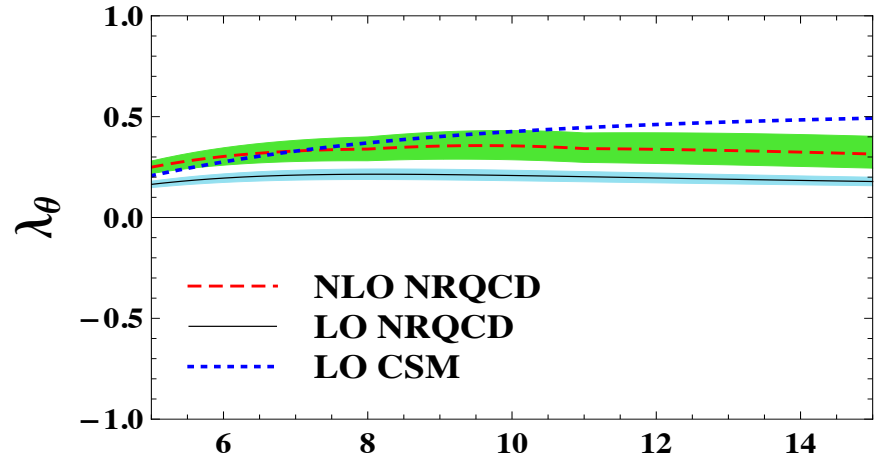
$\sqrt{S} = 7 \text{ TeV}$
 $|y| < 2.4$

helicity frame
 χ_{c1} polarization



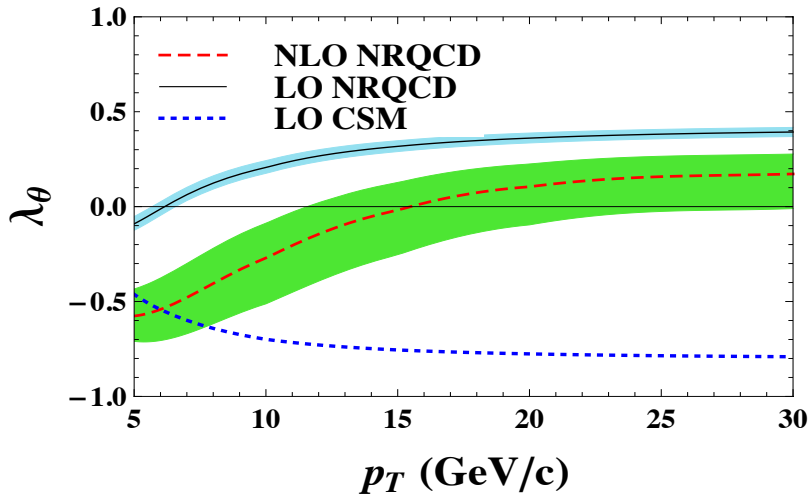
$\sqrt{S} = 7 \text{ TeV}$
 $2 < |y| < 4.5$

helicity frame
 χ_{c1} polarization



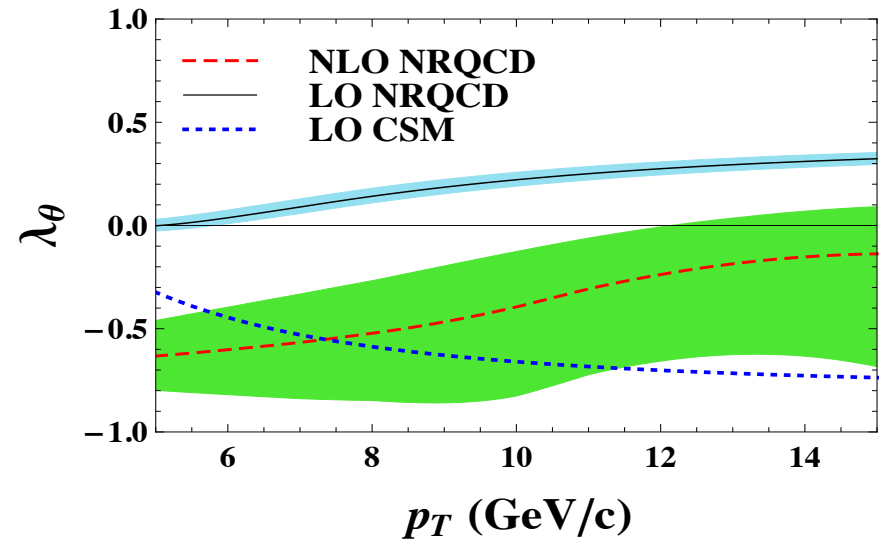
$\sqrt{S} = 7 \text{ TeV}$
 $|y| < 2.4$

helicity frame
 χ_{c2} polarization

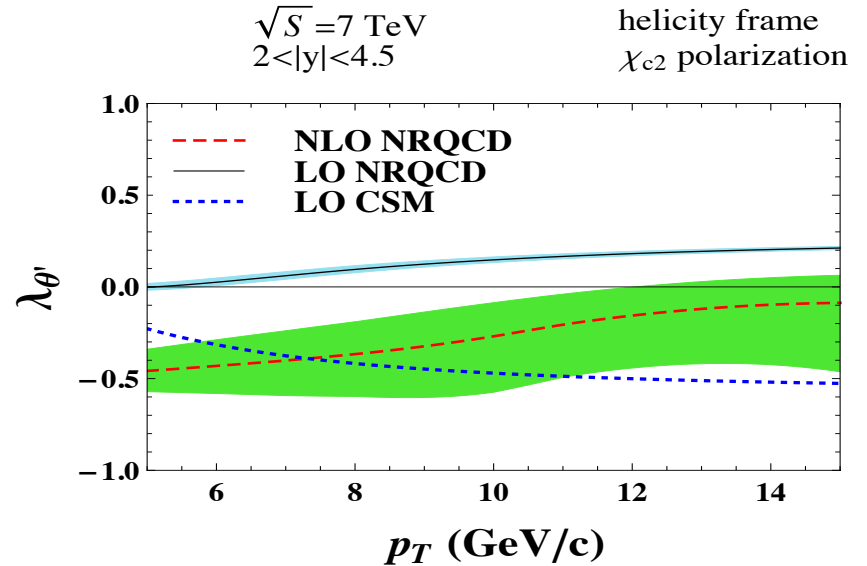
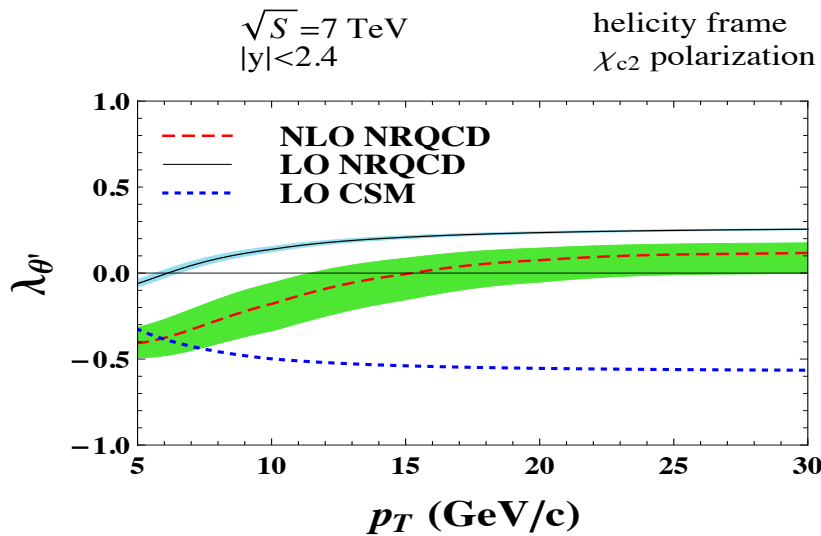
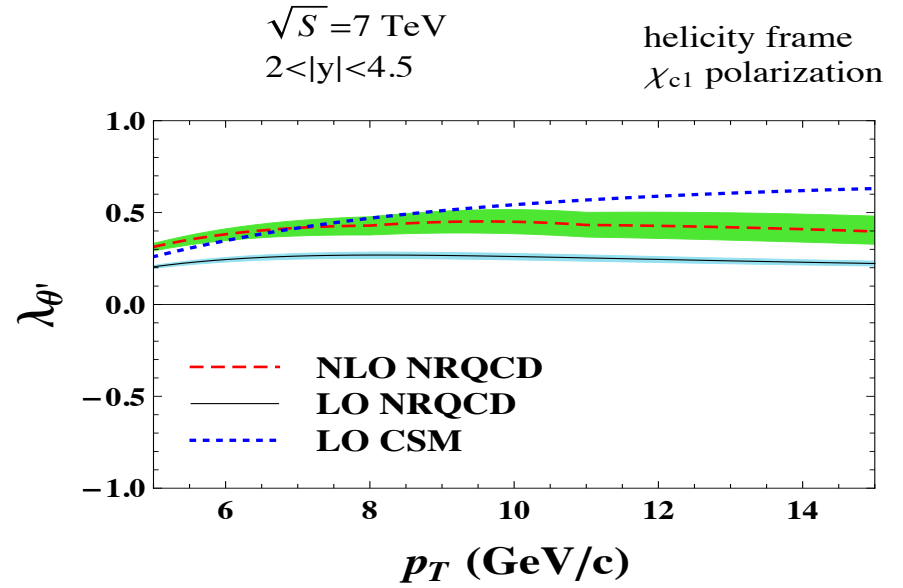
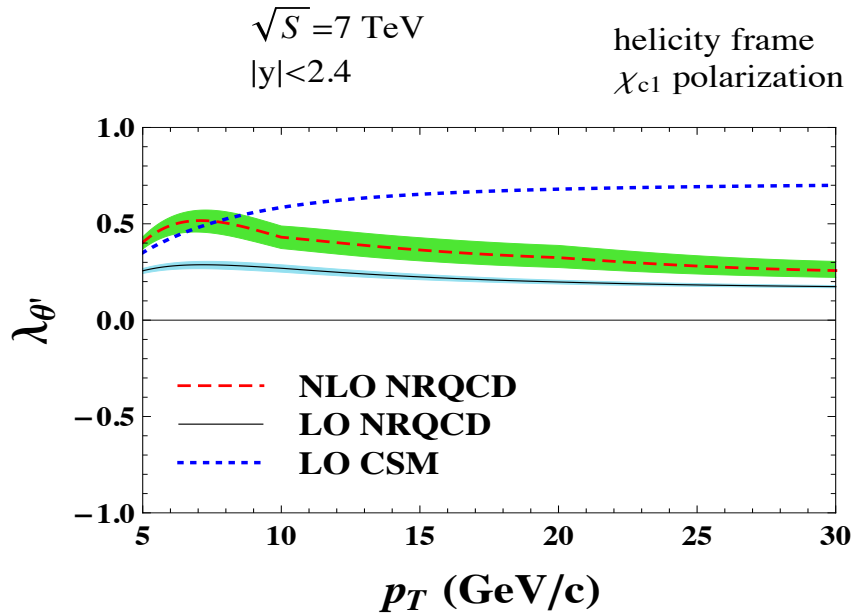


$\sqrt{S} = 7 \text{ TeV}$
 $2 < |y| < 4.5$

helicity frame
 χ_{c2} polarization



$\chi_{cJ} > J/\psi \quad \gamma > l^+ l^- \quad \gamma$



Conclusion

- Kinematical enhancement of NRQCD amplitudes in hadroproduction p_T spectrum motivated us to do complete NLO level analysis.
- It seems that hadroproduction J/ψ (not ψ') data are still compatible with NRQCD prediction as long as S-wave and P-wave cancellation is sufficient (fine tuning??).
- However, our fit is still in disagreement with photo-production data and BELLE data. Hence, we also compare with other groups' fit.
- **There is no consistent solution between NRQCD factorization, hadroproduction (polarization and yield) data, photoproduction data, two-photo production data, BELLE data at NLO-level.**
- Moreover, χ_{cJ} polarization at NLO level is presented.

Back up slides

r0 and r1

\sqrt{S} (TeV)	region of y	r_0	r_1
1.96	(0 ,0.6)	3.9	-0.56
7	(0 ,0.75)	4.0	-0.55
7	(0.75,1.50)	3.9	-0.56
7	(1.50,2.25)	3.9	-0.59
7	(0 ,2.4)	4.1	-0.56
7	(0 ,1.2)	4.1	-0.55
7	(1.2,1.6)	3.9	-0.57
7	(1.6,2.4)	3.9	-0.59
7	(2.5, 4)	3.9	-0.66
7	(2 ,2.5)	4.0	-0.61
7	(2.5, 3)	4.0	-0.65
7	(3 ,3.5)	4.0	-0.68
7	(3.5, 4)	4.0	-0.74
7	(4 ,4.5)	4.2	-0.81
14	(0 , 3)	3.9	-0.57
0.2	(0 , 0.35)	3.8	-0.60
0.2	(1.2 , 2.4)	4.0	-0.66